Military Technical College
Kobry El-Kobbah,
Cairo, Egypt.

15th International Conference on Applied Mechanics and Mechanical Engineering.

THERMOMECHANICAL FATIGUE BEHAVIOR OF BURNISHED 7075–T6 ALUMINUM ALLOY

A. A. Abo El-Nasr*

ABSTRACT

This paper presents the results of series of isothermal and thermomechanical fatigue (TMF) tests of unburnished and burnished 7075-T6 Al specimens. A designed roller burnishing tool was employed to improve the strength of the surface layer of the fatigue specimens. The fatigue stresses were developed in the specimens by combining constant amplitude rotating bending stresses along with constant temperature variation. Isothermal (ITF) and TMF tests were conducted on a rotary bending fatigue testing machine. In ITF tests, two different constant temperatures were used namely: 523 and 623 K. For TMF tests, a constant temperature variation between 523 and 623 K was applied. All these tests were conducted at a constant operating speed of 1200 rpm.

The present results revealed that roller burnishing processes have played a significant role in increasing the fatigue lifetimes for both ITF and TMF specimens. The enhanced fatigue strength of the burnished specimens was attributed to the overall increase in the surface layer strength which may delay fatigue crack growth from the surface. Two distinct fatigue fracture regions were observed: region I and region II. In region I, the fracture surface is associated with the formation of fatigue striations. In region II, the fracture surface is covered with surface dimples. This indicates that local strain softening mechanism has dominated the final stage of fatigue failure. Extensive effort has been paid at investigating the fracture surface of ITF and TMF specimens.

KEY WORDS

Thermomechanical fatigue, 7075-T6 Al, Fatigue lifetime, Burnishing, Fracture

* Associate Professor, Dpt. of Mech. Engineering, College of Engineering, Qassim University, Buraidah 51452, Saudi Arabia, On leave from Dpt. of Production Engineering and Mechanical Design, Faculty of Engineering, Menoufiya University, Shebin El-Kom, EGYPT

INTRODUCTION

Thermomechanical fatigue (TMF) is one of important phenomena deciding upon the cracking processes in machine components exposed to mechanical and thermal influences in aviation and transport [1,2]. In such applications, most of the mechanical components are constrained and not free to strain in response to variations in mechanical and thermal stresses. These types of components are more likely to endure variable or randomly amplitude of cyclic loading and temperature, whilst in service [3,4]. The evolution of microstructure and micro-mechanisms of degradation differ from that encountered in monotonic deformation or in isothermal fatigue (ITF) [5]. Under operating conditions, component lifetime may not be limited by strength as the primary design parameter, but lifetime may be limited by various damage mechanisms such as fatigue, creep or oxidation, which can act indecently in combination [6]. Fatigue damage, for example, is generated by cyclic loadings and the process is primarily time independent. When these damage mechanisms act in condition, a creep-fatigue-oxidation interaction exists [7]. Therefore the component undergoing such conditions must possess highly mechanical and thermal properties especially under elevated and ambient temperatures.

Burnishing processes of mechanical parts is a surface enhancement means in which plastic deformation of surface irregularities occurs by exerting pressure through a very hard and smooth roller or ball on a surface to generate a uniform and work-hardened surface layer [8]. This technique overcomes the complications associated with the machined surfaces produced by conventional machining processes such as turning and milling that have inherent irregularities and defects like tool marks and scratches which cause energy dissipation and surface damage [9]. Besides producing a good surface finish, burnishing has additional advantages over other surface enhancement techniques, such as securing increased hardness, corrosion resistance and fatigue lifetime due to the generated compressive residual stress in the surface layer. The developed residual stresses are probably the most important aspect in assessing surface integrity because of their direct impact on the performance of the mechanical parts in service [10,11]. Furthermore, roller burnishing has been found to improve the surface roundness and dimensions stability [12].

Fatigue lifetime and fracture of the mechanical components depend primarily on loads, material, geometry and environmental effects. Its evolution is generally based on tests of three forms of fatigue loadings: isothermal strain-controlled low cycle fatigue (LCF) tests, TMF tests, and thermal shock tests [13]. Extensive research efforts have been devoted on studying fatigue of 7075 Al alloy under isothermal conditions which have contributed significantly to knowledge of the general features of fatigue failure under high temperatures [8-10,14]. This alloy has been the focus of a number of experimental studies due to its technological importance [9,10]. These studies are of great importance from technical point of view, since this alloy is widely used in applications at intermediate temperatures. On this basis, not only measuring the elevated temperature ITF behavior is essential, but also a study of TMF behavior is necessary. Although a large number of studies have dealt with TMF behavior under tension-tension and tension-compression for many alloys from mechanical and microstructural point of view [8-12], there is a lack of systematic studies on the fatigue behavior of 7075-T6 Al, especially under rotating bending TMF conditions.

The objective of this work is to investigate TMF behavior of burnished and unburnished 7075-T6 Al specimens. For the purpose of comparison, basic data of ITF of the alloy will be measured at 523 K and 623 K. Attempts will be made to study the fracture behavior of TMF by using SEM with reference to ITF behavior.

EXPERIMENTAL PROCEDURES

Material and Test Specimen

The material used in this work was 7075-T6 Al alloy (7075-T6 Al). High strength precipitation hardening 7xxx series of the aluminum alloys, such as 7075 are used extensively in aerospace, turbines and nuclear industries. The chemical composition of the alloy used in this work is given in Table 1. The alloy was fabricated by casting technique and was delivered in the form of extruded cylindrical bars with a diameter of 12 mm. Cylindrical test specimens were machined from the as received bars with identical dimensions, shown in Figs. 1(a and b). Burnished and unburnished 7075-T6 Al specimens were fatigue tested under ITF and TMF conditions. The main mechanical properties of the alloy is σ_{ult} = 540 MPa and σ_y = 480 MPa [14].

Table 1. Chemical composition of 7075-T6 Al alloy used in this work.

Element	Zn	Mg	Cu	Fe	Cr	Mn	Al
Weight (%)	5.5	2.5	1.5	0.25	0.20	0.2	Balance

Burnishing Process

A roller burnishing tool was designed and fabricated from a high strength Nickel-Chromium super alloy. The roller, as shown in Fig. 2.a, contains two sections, with a total length of 7 mm; the first has a conical outside surface with a cone angle of about 7° and the other has a normal cylindrical surface. The tool is designed in such a way to burnish the surface in two stages. The first is to deform a very thin surface layer and the final one is to iron the deformed layer. The roller is supported by a sufficient pressure to keep its depth constant and is free to roll on the surface of the specimen [10]. Fig. 2.b shows a photo of the burnishing tool which is firmly clamped on a general lathe machine. The roller is always in mechanical contact with the surface to be burnished. So that, with roller lateral motion, the surface is covered with a series of overlap passes to achieve maximum compression with minimum cold working. The burnishing parameters remain constant for all the specimens used, see Table 2 [15]. A single burnishing pass process was applied to the specimens. More details regarding the burnishing process are found elsewhere [10,14].

Table 2. Burnishing parameters used in the present burnishing operations.

Burnishing Force, N	Burnishing Speed, rpm	Burnishing Feed, mm/rev	Max. Roller Contact width, (mm)
235	523	0.1	~7

Suitable mineral oil was used for the purpose of cooling and improving the tribological behavior during the process. Surface roughness of burnished samples was measured by using a Surftest-402 system. The average surface roughness of the samples, before and after burnishing, was found to be ~2.25 μm and ~1.14 μm, Ra, respectively.

Fatigue Testing and Fracture Surface Investigation

ITF and TMF tests were conducted in an open furnace using a Rotating Bending Fatigue Testing Machine (Model H7), Shimadzu Co., Kyoto, Japan, shown in Fig. 3.a. A separate unit was connected with the furnace controller to adapt the temperature variation for developing TMF tests. Three sets of tests were designed for fatigue testing under constant amplitude fatigue stresses ranged from ~ 120 to ~ 350 MPa, two of them are ITF tests at temperatures of 523 K and 623 K (±2K) and the third one is TMF tests at cyclic temperature between 523 and 623 K with a trapezoidal waveform, Fig. 3.b. A thermal load, with trapezoidal waveform, with heating and cooling rates of ±1.11 $K.s^{-1}$ and high-and low-temperature holding times of 60 sec., was applied. The whole thermal cycle takes ~5 minutes. All fatigue tests were conducted at a constant speed, 1200 rpm. Some points on S-N curves represent the average value of at least three data points. The fatigue curves were determined by measuring the number of cycles to failure, N, at each constant bending fatigue stress, S. The bending fatigue stress was calculated according to the applied bending moment, M, and diameter of the gauge length of the specimen, d, assuming that the specimen stays in elastic condition through its fatigue lifetime. It is expressed as:

$$S = (M.r)/I \quad ; r = (d/2), \text{ and } I = (\pi.r^4/4) \qquad (1)$$

Fracture surfaces of some broken specimens were investigated by using scanning electron microscopy (SEM), Hitachi SU-70 UHR FE-SEM. These investigations were made in order to gain more understanding of the fracture mechanism that governs TMF behavior of the present alloy.

EXPERIMENTAL RESULTS AND DISCUSSIONS

ITF and TMF Behaviors

Figure 4 shows the S-N curves of unburnished 7075-T6 Al specimens, on semi-logarithm scale, for three sets of fatigue data where the fatigue stress is plotted against number of cycles to failure. The figure presents the results of two sets of ITF data obtained at 523 K and 623 K and that of one set of TMF data tested at temperature alternated between 523 and 623 K. For ITF, there are small differences in the fatigue lifetimes of the specimens tested at 523 K and those tested at 623K, where the higher the temperature the lower the fatigue lifetime. It appeared from these results that this alloy keeps its good strength at these high temperatures. However, for TMF in Fig. 4, it clearly indicated that the fatigue lifetime deceased significantly compared with that of ITF conditions. For example, at fatigue stress equal to 200 MPa, the fatigue lifetime for ITF specimens tested at 623 K decreased from ~$2.2x10^5$ cycles to be ~$1x10^5$ cycles for TMF specimens. This decrease in fatigue lifetime may be attributed to the increase in material's brittleness that developed due to the interaction between thermal and mechanical loadings which

eventually makes the material loses gradually its toughness [1,14]. In this situation, temperature variations will produce damaging thermal stresses and strains across the specimen in a complex way which limit the lifetime of the specimens. These observations were supported by the fractographic findings in the following section.

Figure 5 shows the S-N curves for burnished 7075-T6 Al specimens under same testing conditions of Fig. 4. Similar trends of fatigue strength to that in Fig. 4, with a reasonable increase in this fatigue strength, are obtained in Fig. 5. These results reveal that roller burnishing process has generally improved the fatigue strength for all studied cases. For example, for fatigue lifetime of $1x10^5$ cycles, the fatigue strength increased from ~195 MPa for unburnished TMF specimens to be ~220 MPa for burnished TMF specimens. Also, for TMF specimens tested at 225 MPa, the fatigue lifetime increases from ~$7.5x10^4$ cycles for unburnished specimens to be ~$9.5x10^4$ cycles for the burnished specimens. This increase in fatigue lifetime is attributed to the increase in fatigue strength of the surface layer as a result of the application of burnishing process to the present specimens [9,10]. It is believed that application of roller burnishing processes on 7075-T6 Al specimens have introduced a significant amount of compressive residual stress into a surface layer of about 0.4 mm. The presence of residual stress in the surface layers may be a good reason for this improvement. The development of compressive residual stresses will partially or completely compensate the induced tensile stresses that simultaneously exist in rotating bending fatigue specimens [10,16].

The relationship between fatigue stress, S, and fatigue lifetime, N, for all the cases, was obtained by applying power fitting method on the fatigue data, as follows:

$$S = A.N^B \quad (2)$$

where A and B are constants depend on material and test conditions and their values were estimated from the fitting of S-N curves and they are given in Table 3.

Table 3. Values of A and B in Eq. 2 obtained from power fitting of fatigue data.

	Unburnished Fatigue Specimens			Burnished Fatigue Specimens		
	ITF (523 K)	ITF (623 K)	TMF (523-623 K)	ITF (523 K)	ITF (623 K)	TMF (523-623 K)
A	8.742	8.868	9.336	8.449	8.285	8.115
B	-0.276	-0.293	-0.352	-0.242	-0.234	-0.237

Fractographic Observations

The fracture surfaces of 7075-T6 Al specimens have been examined using SEM. Fig. 6 and Fig. 7 show SEM fractographs for burnished ITF and TMF specimens, respectively. Both of these two specimens were tested under ~225 MPa. In Fig. 6.a, the fatigue fracture exhibited two distinct regions: region I and region II. Region I represents the crack initiation and propagation stage. In this region as shown in Fig. 6.b, the fracture surface is associated with the formation of fatigue striations. These striations were formed as the crack propagates through the specimen cross section during opening and closing the crack whilst the specimen rotates. Fatigue striations are the most common feature of fatigue fracture of 7075-T6 Al and they can only be seen on a microscopic scale. The size and density of these striations indicate the

amount of plasticity that have undergone through the crack growth. It has been established that each striation is associated with the crack growth during one complete loading cycle. The crack propagation direction is generally normal to striations lines [17]. The specimen, in region II, was fractured in a different manner from that of region I where the cross section was no longer able to withstand the applied stress, shown in Fig. 6.c. The fracture surface is covered with deep and thick walled dimples. The features of these dimples indicate that local strain softening mechanism has dominated the final stage of fatigue failure.

The fracture characteristics of a burnished TMF specimen tested at 225 MPa are shown in Figs. 7. It is obvious in Fig. 7.a that the fracture of TMF specimen has an irregular surface in comparison with that of ITF specimen. Fatigue striations have been formed in the outer ring on the fracture surface representing the crack growth region, region I, as shown in Figs. 7.b. Another common feature associated with the formation of fatigue striations is the existence of secondary cracks on the fracture surface, pointed by arrows in Fig. 7.a. The direction of main crack propagation depend on the nature of applied loading and microstructure features through which the crack is advancing and this causes the striations to alter orientation locally. Although, the temperature variation of TMF was not very large, 100 K, TMF tests have led to more dangerous fatigue fracture than that of ITF specimens. The brittle character of the fracture appearance can be easily recognized by the typical cleavage facets presented on the fracture surface of specimen. This finding is supported by nature of the surface dimples that were formed in final stage of fracture, region II. These dimples are shallow and have fine wall thickness which indicates that they were formed in the very late stage of fatigue lifetime. This situation corresponds to the situation in which the material is subjected to periodically creep-fatigue interaction [7]. It is believed that crack initiation and further propagation tended to behave in a transgranular manner. These microstructural observations indicate also that failure of TMF specimens is dominated by fatigue damaging mechanism whatever the temperature situation.

It is well established that fatigue fracture is particularly insidious because it occurs without any obvious warning. This can be seen in the fractographs where the appearance of the fracture surface revealed a transgranular features with very limited plastic deformation. For bending loading, the maximum normal stress is parallel to the specimen axis and keeps varying from a tensile value on one surface to zero at the center to a compression value on the other surface. In this situation, the main crack occurs on a plane normal to the axis of the specimen and proceeds from the tensile side to the opposite side. This is very clear in Figs. 6 and 7, where fatigue striations have been formed on the outer ring of the fracture surface and propagated across until separation occurred in the interior section of the specimens [14,18]. It is evident based on these findings that the fracture mechanism was characterized with a crack initiation and propagation region followed by a transgranular final region. In crack propagation region, many striations were found as shown in Figs. 6.b, and 7.b, indicating that the crack propagation, in this stage of fatigue life, occurred by fatigue fracture. In the transgranular region, no striations were observed but surface dimples, due to cavity nucleation and growth, Figs. 6.d, and 7.d. These surface dimples indicate that local strain softening has dominated the final stage of fatigue. The existence of strain softening caused ratcheting strain and the accumulated ratcheting strain can then produce additional damage [17]. It is

evident also that the main role of the present burnishing process was to decrease the surface irregularities which minimize the potential sources of crack initiation and consequently delays the crack initiation stage. This process has affected only the fatigue lifetime and its effect on the fatigue fracture mechanism has less importance. Additional data on fatigue behavior of 7075-T6 Al should be obtained in order to cover wide range of TMF parameters, including the experiments of high and low cycle fatigue as well as a wide range of temperature intervals.

CONCLUSIONS

The experimental results and their discussions for burnished and unburnished 7075-T6 Al specimens tested under ITF and TMF have led to the following conclusions:

1. The present roller burnishing processes have introduced a significant improvement in fatigue strength for both ITF and TMF specimens. This enhancement in fatigue strength was attributed to the overall increase in surface layer strength which may delay fatigue crack growth from the surface. The relationship between fatigue stress, S, and lifetime, N, under ITF and TMF conditions can be expressed using an empirical equation; $S = A.N^B$, where A and B are constants. It is found that the existence of TMF resulted in a significant decrease in fatigue strength of compared to ITF specimens. Small difference in the fatigue lifetime was obtained between the two kinds of ITF testes at 523 K and 623 K.
2. The fracture surface is characterized, for ITF and TMF cases, by two distinct regions: I and II. The fracture surface in the former region is associated with the formation of fatigue striations that were formed as the crack propagates through the specimen cross section whilst the specimen rotates. In the later region, fracture surface is covered with surface dimples indicating that local strain softening mechanism has dominated the final stage of fatigue failure.
3. It is believed that crack initiation and further propagation tended to behave in a transgranular manner. For TMF specimens, fatigue cracks were observed on the fracture surface and final failure tends to be brittle. Microcracks were also observed and many of them were larger than those in the case of ITF specimens. Although, the temperature variation of TMF was not very large, 100 K, the TMF tests have led to more dangerous fatigue fracture compared to ITF tests. These microstructural observations indicate also that failure of TMF specimens is dominated by fatigue damaging mechanism.

ACKNOWLEDGMENT

The author is gratefully thanks *Dr. Robert Steffen*, Product Applications Manager, Hitachi High-Technologies Europe GmbH, 47807 Krefeld, Germany, for running SEM investigations at his Lab in Germany. This work is partially supported by the deanship of scientific research at Qassim University, Project no. SRD-008-83.

REFERENCES

[1] Sehitoglu, H., "Thermal and Thermo mechanical Fatigue of Structural Alloys, Fatigue and Fracture", ASM Handbook, Vol. 19, pp 527-556, (1996).

[2] Okrajni, J., Mutwil, K., Ciesla, M., "Chemical pipelines material fatigue", J of Materials Processing Technology, Elsevier, 164-165, 897-904, (2005).

[3] "Thermomechanical Fatigue Behavior of Materials", *Eds*. J. Bressers, S. Kalluri, M.A. McGaw, ASTM Inter., 4th Vol., pp 240-523, (2003).

[4] Okrajni, J., Marek, A., Junak, G., "Description of the deformation process under thermo-mechanical fatigue", J. of Achievements in Materials and Manufacturing Engineering, Vol. 21 Issue 2, April, pp 15-24, (2007).

[5] Shi, H-J., Korn, C., and Pluvinage, G., "High Temperature Isothermal and Thermo-mechanical Fatigue on a Molybdenum-Based Alloy" Materials Science and Engineering A247, pp 180-186, (1998).

[6] Mannan, S.L. and Valsan, M., "High-temperature low cycle fatigue, creep–fatigue and thermo-mechanical fatigue of steels and their welds", Inter. J Mechanical Sci., Vol. 48, Issue 2, pp 160-175, Feb. (2006).

[7] Zauter, R., Petry, F., Christ, H.-J., and Maghrabi H., "Thermo-mechanical Fatigue of the Austentitic Stainless Steel AISI 304L" Thermo-mechanical Fatigue Behavior of Materials, ASTM STP 1186, H. Sehitoglu, *Ed*., Philadelphia, pp 70-90, (1993).

[8] Zinn, W. and Scholtes, B. "Mechanical Surface Treatments of Light Weight Materials – Effects on Fatigue Strength and Near-Surface Microstructures", J. of Mater. Eng. & Performance, Vol. 8 (2), pp 145-157, April (1999).

[9] El-Tayeb, N.S., Low K.O. and Brevern P.V., "Environmental effects on low cycle fatigue of 2024-T351 and 7075-T651 aluminum alloys", Tribology Inter., Vol. 42, pp 320–326, (2009).

[10] Abo El-Nasr A.A., "Fatigue Resistance of Corroded 7075 Al Alloy after Roller Burnishing Processes" 5th Int. Conf. on Mechanical Engineering and Advanced Technology for Industrial Production, (MEATIP 5), Assiut, Egypt, pp 153-161 March 29-31, (2011).

[11] El-Khabeery, M.M. and El-Axir M.H. "Experimental techniques for studying the effects of milling roller-burnishing parameters on surface integrity", Inter. J of Machine Tools & Manufacture, Vol. 41, pp 1705–1719, (2001).

[12] El-Axir M.H. and El-Khabeery M.M., "Influence of orthogonal burnishing parameters on surface characteristics for various materials, J. Mater. Process Tech., Vol. 132, pp 82-89, (2003).

[13] Skelton R.P. and Webster, G.A. "History effects in the cyclic stress-strain response of a polycrystalline and single crystal nickel-base Superalloy. Mater. Sci. Engen., Vol. A 216, pp 139-154, (1996).

[14] Abo El-Nasr, A.A., Ayad, M., and Fattouh, M., "High Temperature Fatigue of 7075 Aluminum Alloy Via Low Plasticity Burnishing", Engineering Research Journal (EJR), Faculty of Engg., Menoufiya University, Shebin El-Kom, Egypt, V. 25, No. 2, pp 135-145, April (2002).

[15] Basak, H. and Goktas, H., "Burnishing Process on Al-Alloy and Optimization of Surface Roughness and Surface Hardness by Fuzzy Logic", Materials and Design, Vol. 30, pp 1275-1281, (2009).

[16] DuQuesnay D.L. and Underhill, P.R., "Fatigue Life Scatter in 7xxx Series Aluminum Alloy", Inter. J. of Fatigue 32, pp 398-402, (2010).

[17] Verma, B.B., Atkinson, J.D. and Kumar, M., "Study of Fatigue Behavior of 7475 Aluminum Alloy", Bull. Mater. Sci., Vol. 24, No. 2, pp 231-236, April (2001).

[18] Payne, J., Welsh, G., ChristJr, R.J., Nardiello, J., Papazian, J.M., "Observations of Fatigue Crack Initiation in 7075-T651", Inter. J. of Fatigue, Vol. 32, pp 247-255, (2010).

FIGURES:

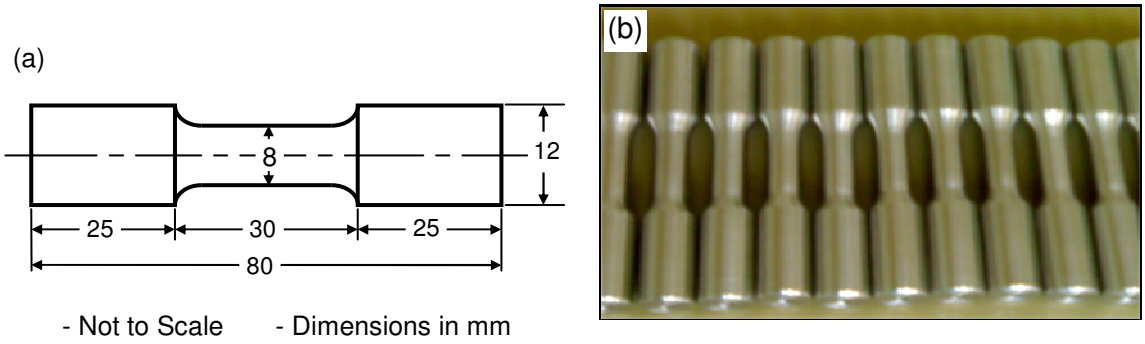

Fig. 1. (a) Schematic draw of fatigue test specimen and (b) Some of burnished specimens used in the present work.

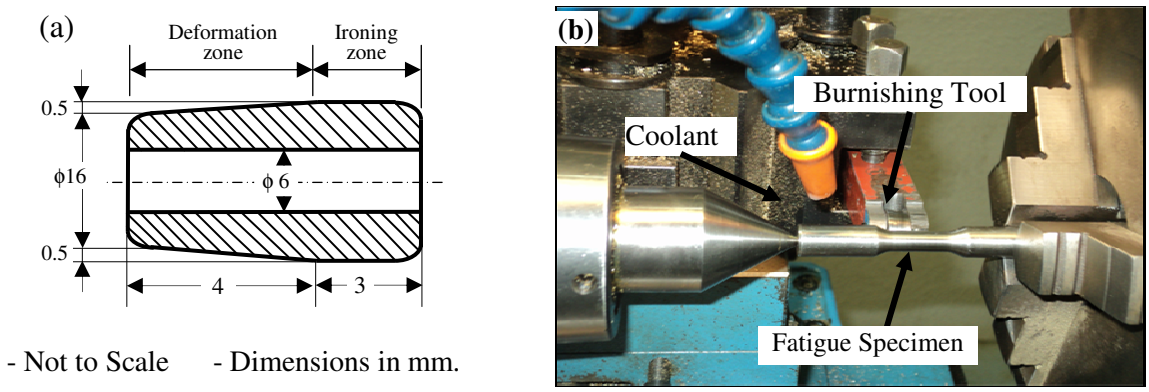

Fig. 2. (a) Schematic draw of the roller of the burnishing tool and (b) A photograph of the burnishing set-up on a general lathe machine prior the burnishing process.

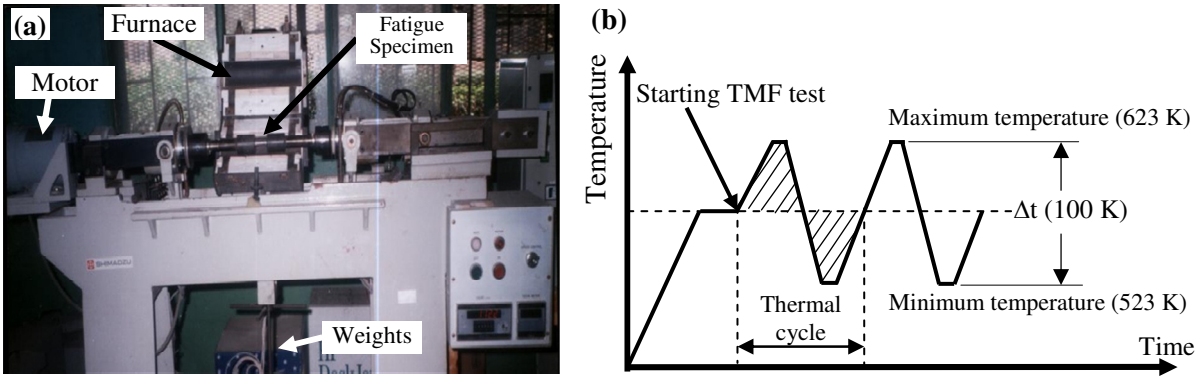

Fig. 3. (a) Fatigue Testing Machine used in this work and (b) Schematic draw of thermal load history.

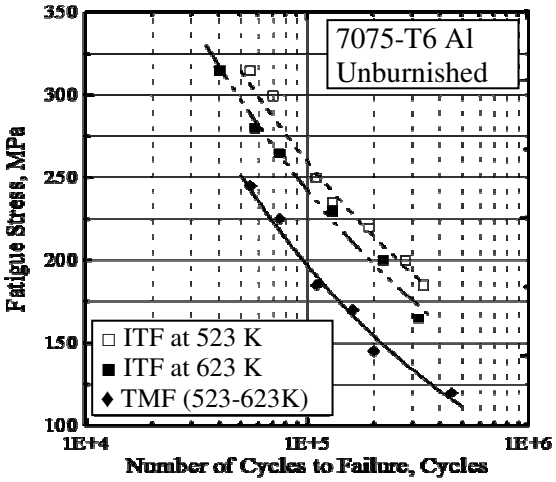

Fig. 4. ITF and TMF lifetimes *vs* bending fatigue stresses for 7075-T6 Al unburnished specimens.

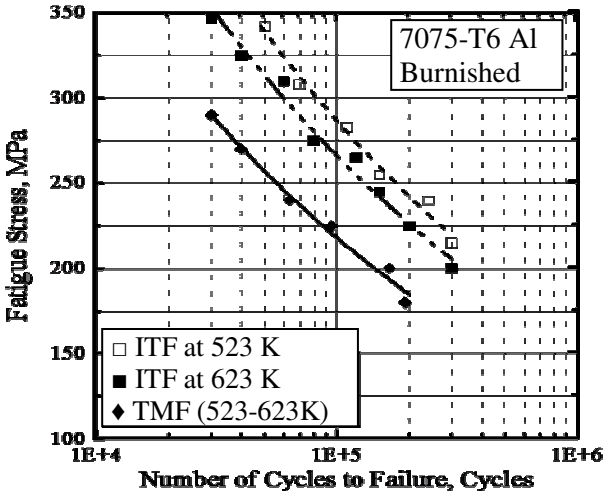

Fig. 5. Fatigue lifetimes *vs* bending fatigue stresses for burnished 7075-T6 Al burnished specimens.

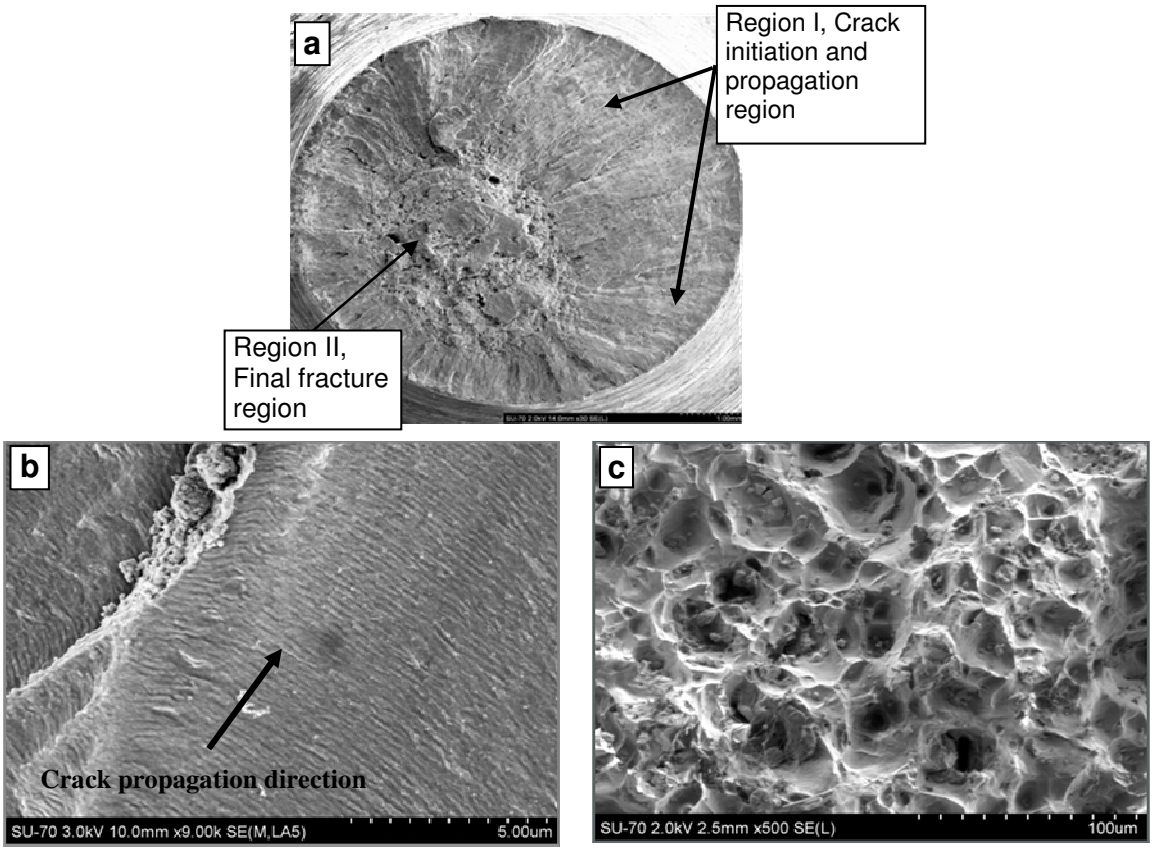

Fig. 6. SEM fractographs of burnished 7075-T6 Al ITF specimen tested under ~225 MPa at 623 K (a) Overview of fatigue fracture surface, (b) region I, fatigue striations, arrow point to crack propagation direction and (c) region II, final fatigue fracture.

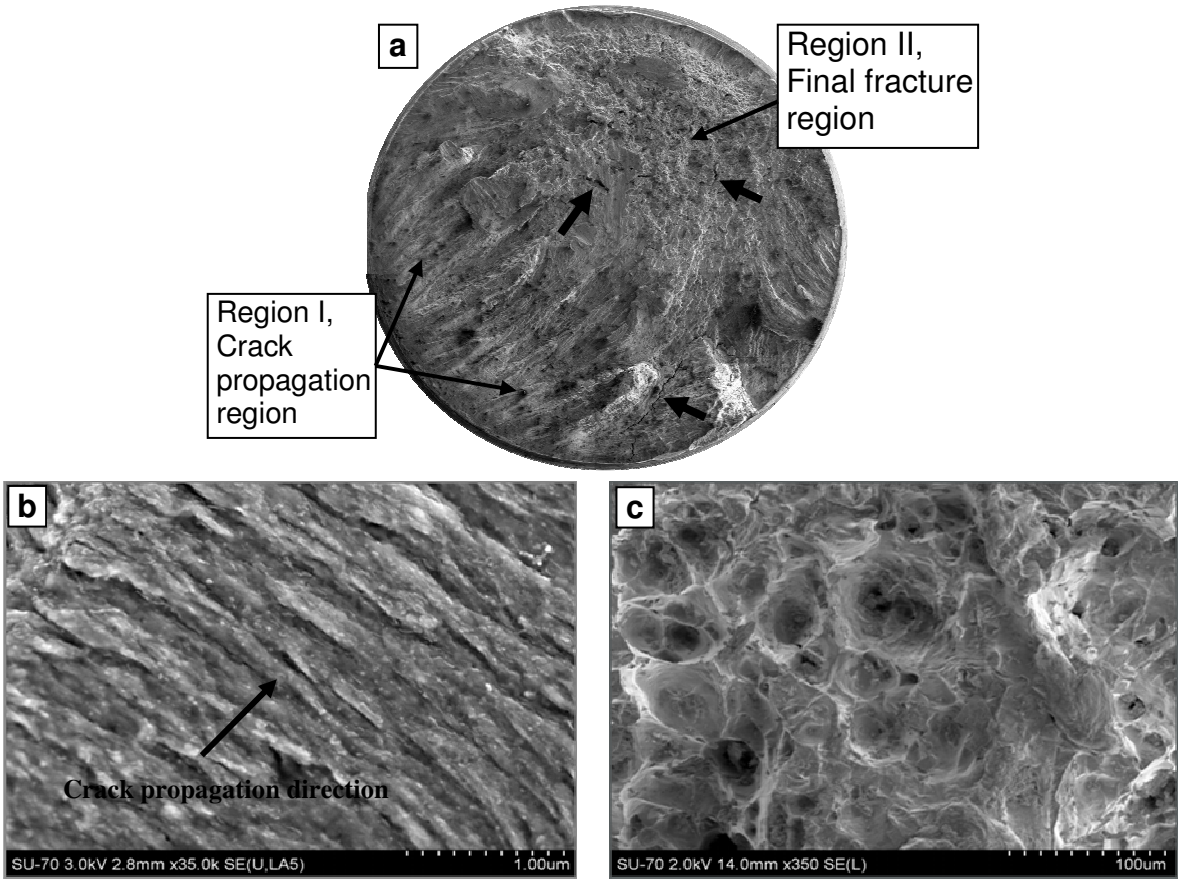

Fig. 7. Typical fatigue fracture surfaces of burnished TMF specimen failed under stress ~225 MPa, (a) Overview of fracture surface, (b) region I, fatigue striations, arrow point to crack propagation direction and (c) region II, final fatigue fracture.